Accepted Manuscript

Spectroscopic and Photophysical Studies of a Naphthalene-Based Emissive Probe for Metal Cations

Catherine S. de Castro, J. Sérgio Seixas de Melo, Adrián Fernández-Lodeiro, Cristina Núñez, Carlos Lodeiro

Please cite this article as: Catherine S. de Castro, J. Sérgio Seixas de Melo, Adrián Fernández-Lodeiro, Cristina Núñez, Carlos Lodeiro, Spectroscopic and Photophysical Studies of a Naphthalene-Based Emissive Probe for Metal Cations, *Inorganic Chemistry Communications* (2014), doi: 10.1016/j.inoche.2014.07.007

Spectroscopic and Photophysical Studies of a Naphthalene-Based Emissive Probe for Metal Cations
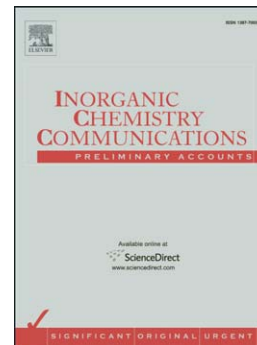
Catherine S. de Castro,[a] J. Sérgio Seixas de Melo,[a*] Adrián Fernández-Lodeiro,[b,c] Cristina Núñez,[b,d,e] Carlos Lodeiro[b,c*]

[a] Coimbra Chemistry Center, Department of Chemistry, University of Coimbra, 3004-535 Coimbra, Portugal.

[b] BIOSCOPE Group, REQUIMTE-CQFB, Chemistry Department, Faculty of Science and Technology, University NOVA of Lisbon, 2829-516 Campus de Caparica, Portugal.

[c] ProteoMass Scientific Society. Madan Parque. Rua dos Inventores. 2825-182. Caparica. Portugal

[d] Ecology Research Group, Department of Geographical and Life Sciences, Canterbury Christ Church University, CT1 1Q U, Canterbury, United Kingdom

[e] Inorganic Chemistry Department, Faculty of Chemistry, University of Santiago de Compostela, 15782 Santiago de Compostela, Spain

Corresponding Authors: *E-mail: sseixas@ci.uc.pt (J.S.S.d.M.), cle@fct.unl.pt (C.L.).

Abstract

A comprehensive photophysical characterization of a bis-naphthalene derivative, **L**, was carried out in acetonitrile, using UV-Vis absorption, steady-state and time-resolved emission spectroscopy. It was found that in the 250-400 nm region, the absorption spectra showed two bands with maxima at ~ 220 nm and ~292 nm whereas the emission spectrum showed a band settled between 300 and 550 nm. A detailed time-resolved investigation (in the ps and ns time domain) showed that the fluorescence decay of **L** in dichloromethane was bi-exponential indicative of the presence of a ground-state equilibrium involving two species: monomeric (absorption of a single naphthalene unit) and dimeric. Upon addition of Cu^{2+}, Zn^{2+}, Cd^{2+} or Hg^{2+} metal cations in acetonitrile a quenching of the fluorescence emission was observed. From time-resolved data, it is shown that the fluorescence contribution of the species with the longest decay time was sensitive to the explored metal ions.

Keywords: Naphthalene; chemical probes; metals; fluorescence quenching; time-resolved fluorescence; dimer.

Metal cations are important for the functioning of the organism; however, when in excess they can cause serious health problems. In particular, excess of copper can cause severe health problems such as irritation, headaches, dizziness, nausea and diarrhea when ingested in small (yet excessive) amounts and ultimately can lead to liver, kidney damage and even death in large amounts. In turn, zinc in excess is associated with epilepsy, Alzheimer's and Parkinson's diseases, ischemic stroke and infantile diarrhea [1]. Accumulation of mercury in the body is responsible for several complications such as prenatal brain damage, serious cognitive and motion disorders and Minamata's disease [2] while cadmium can lead to kidney disease, lung damage and fragile bones.

The main source of these metals occurs through contaminated water and food due to pollution of soils and ground-waters. Due to the harmful effects of these metals (and others) and with the ultimate goal is of finding analytical sensors with wide applicability, capable of

1

detecting selectively small amounts of metal cation, preferably cheap and recoverable for subsequent application, more accurate ways to detect and determine their concentrations have been the subject of recent investigations.

Molecular scale sensors (probes) emerge within this type of molecules; they consist in compounds that when interact with a given analyte cause a chemical change which in turn induces a change in a measurable property. Depending on the measurable property, the probe can be classified as electrochemical, electronic, optic, etc. From these, particular attention must be given to the optic sensors, i.e., sensors that cause changes in optical parameters such as absorption, luminescence (fluorescence and/or phosphorescence), refractive index, etc. Within these parameters, inducing changes in the fluorescence emission is one of the more advantageous since fluorescence spectroscopy is highly sensitive, it is easily performed [3], it does not require a reference nor the analyte is consumed [4], it has a quick response [5] and different assays can be designed based on different aspects of the fluorescence output (lifetime, intensity, anisotropy and energy transfer) [4].

The interaction of a ligand to an analyte can induce several changes as (red or blue) shifts of the maxima band (from the absorption or/and emission spectra) which can induce color changes in the visible region, quenching or enhancement of the fluorescence spectra, appearance or disappearance of bands, etc. This changes can be caused by different mechanisms such as photoinduced electron or charge transfer (PET or PCT) [6,7], excimer or exciplex formation [8-10], fluorescence resonance energy transfer (FRET) [11], internal charge transfer (ICT) [12,13], excited state intramolecular proton transfer (ESIPT) [14,15], etc [16].

The synthesis of chemical probes highly sensitive and selective to the detection of transition metals (M) such as Cu^{2+}, Zn^{2+}, Cd^{2+} and Hg^{2+} ions has increasingly attracted the attention of several scientific fields [17] in particular medicine and environment [18].

Among the various methods for detecting cations, fluorescence spectroscopy is a technique widely used both for its versatility [6], high sensitivity and selectivity [7,19]. Indeed, the detection ability is associated with the interaction between the unit responsible for the selective binding of ions - ionophore - and the unit which regulates the signal transduction -fluorophore, which may result in an increase/ decrease in the fluorescence intensity of the probe [6]. Several factors make fluorescence one of the most important ways for understanding the mechanisms of chemical events in the scope of recognition, amongst these are the possibility of studying it analytically, since this technique (i) is highly sensitive, (ii) does not consume the analyte, (iii) nor requires a reference [20]. The applications of fluorophores based on the naphthalene chromophore range from biological markers to the development of detection systems and materials for light-emitting diodes. The naphthalene structure has a low molecular weight and its (spectroscopic and photophysical) properties strongly depend on the number, type and position of substituent groups in the ring. Although the unsubstituted naphthalene is poorly fluorescent (ϕ_F= 0.23 in cyclohexane) [21], if electrons donor and acceptor groups are placed, for example, in positions 2 and 6 of the naphthalene ring, a significant increase in fluorescence is obtained by intramolecular charge transfer [22].

An emissive molecular probe bearing two naphthalene units at the extremities was already investigated in the past by some of us [23]. The probe interaction with cations (such as Cu^{2+}, Zn^{2+}, Cd^{2+} and Hg^{2+}) and anions (F⁻, Cl⁻, Br⁻, I⁻ and CN⁻) was explored in DMSO where it showed to be remarkably selective for Cu^{2+} and to interact with CN⁻ and F⁻.

Following our research interest on the design of new emissive compounds [20,24-27] and metal complexes [28-30], in this work, the photophysical properties of another symmetric probe **L**, with two naphthalene units in the extreme as well, was described together with its interaction (aiming chemoselectivity) with Cu^{2+}, Zn^{2+}, Cd^{2+} and Hg^{2+} metal ions in acetonitrile.

Compound **L** was synthesized according to the method previously reported by us [31]. Molecular probe **L** was found to be soluble in dichloromethane, dimethylsulfoxide, N,N'-dimethyl formamide, acetonitrile, ethanol, cyclohexane and dioxane and insoluble in water. In the solid state, **L** presents a brown color but within the concentrations of ligand in the solvents used, the solution is colorless.

The presence of seven, properly positioned, donor atoms (N_4O_2S) in the ligand structure of **L** (Scheme 1) should give strong recognition ability towards different metal ions. In that case, the coordination ability of ligand **L** towards hydrated triflate salts of Cu^{2+}, Zn^{2+}, Cd^{2+} and Hg^{2+} was explored. For the preparation of the complexes [$ML(CF_3O_3S)_2$].xH_2O, ligand **L** (1 equiv.) and $M(CF_3O_3S)_2$.xH_2O (1 equiv.) (M= Cu^{2+}, Zn^{2+}, Cd^{2+} and Hg^{2+}) were mixed in absolute ethanol. After 4h, the solvent was partially removed to *ca.* 5 mL and diethyl ether was infused into the residue resulting on the formation of a powdery precipitate that was separated by centrifugation and discarded [32]. The solid metal complexes were isolated from the evaporation of the remaining solutions. The complexes were characterized by elemental analysis, IR and MALDI-MS spectra [33]. MALDI-MS spectra of the metal complexes display peaks that confirm the formation of these species. In the IR spectra of the complexes, the band due to the [v(C=O)] and [v(N-H)] stretching modes are shifted to higher wavenumbers when compared to its position in the spectrum of the free ligand (IR (cm^{-1}): v= 1430 (C=C)ar, 1666 (C=O), 2980 (N-H)) [31]. Both effects suggest that in solid state the carbonyl and the amine groups presented on compound **L** could be involved in the coordination to the metal ion.
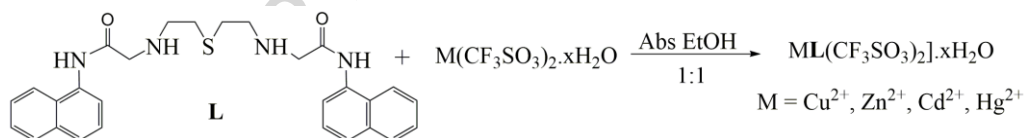
Scheme 1. Synthetic route of the metal complexes derived from **L**.

Figure 1 shows the (normalized) absorption and fluorescence (excitation and emission) spectra of ligand **L** in acetonitrile [34]. Due to its miscibility with water, we select acetonitrile as solvent for the development of the spectroscopic studies of **L**. A single band is observed in the absorption which matches (maxima at the same wavelength) with the excitation spectra collected at λ_{em}= 350 nm. However, the excitation spectrum is broader, clearly mirroring the presence of dimers or higher order aggregates. Very interesting is also to note that the excitation spectra when collected at λ_{em}= 450 nm, presents an "absorption" band between 300 and 425 nm (Figure 1). This is indicative that at longer emission wavelengths the absorption (although with a small molar extinction value) of a dimer is likely to be present. Indeed when exciting at the tail of the absorption band (330 nm) the obtained emission spectra is different than when excitation is at λ_{exc}= 290 nm, see Figure 1 (right hand panel).

The spectral and photophysical properties of **L** are summarized in Table 1 and include the molar extinction coefficient (ε), the fluorescence quantum yield (ϕ_F) and the radiative (k_R) and radiationless (k_{NR}) rate constants in several solvents.

In view of the values in Table 1, it can be seen that the ϕ_F value is low, indicating that the fluorescence is not an efficient route for the deactivation of the excited state of **L**, which is further attested by the small k_F value and high k_{NR} value; moreover, although there are some differences in the ϕ_F and τ_F values, the main deactivation is made through the radiationless deactivation channel ($k_{NR} \gg k_F$). This, however, is not limitative to observe the interaction of this fluorescent ligand with metal cations.

Table 1. Absorption, emission and excitation wavelength maxima (λ_{max}^{abs}, λ_{max}^{em} and λ_{max}^{exc}), together with molar extinction coefficient (ε), fluorescence quantum yield (ϕ_F), fluorescence lifetime (τ_F), and fluorescence and non-radiative rate constants (k_F and k_{NR}) for the probe **L** in dichloromethane at T= 293 K.

Solvent	λ_{max}^{abs} (nm)	λ_{max}^{em} (nm)	λ_{max}^{exc} (nm)[c]	λ_{max}^{exc} (nm)	$\varepsilon_{292\,nm}$ (M^{-1}.cm^{-1})	ϕ_F	τ_F (ns)	k_F (ns^{-1})[g]	k_{NR} (ns^{-1})[h]
CH$_3$CN	290	352[a]	292	297[d]	ND	0.013	0.08[f]	0.163	12.3
CH$_2$Cl$_2$	292	352[b]	296	319[e]	13081	0.009	0.17[f]	0.053	5.8
DMSO	295	354[b]	ND	ND	15040	ND	ND	ND	ND
EtOH	291	351[b]	292	ND	ND	ND	ND	ND	ND

[a]Obtained from the emission spectra collected at λ_{exc}= 285 nm, see Figure 1.

[b]Obtained from the emission spectra collected at λ_{exc}= 281 nm.

[c]Obtained from the excitation spectra collected at λ_{em}= 350 nm, see Figure 1.

[d]Obtained from the excitation spectra collected at λ_{em}= 450 nm, see Figure 1.

[e]Obtained from the excitation spectra collected at λ_{em}= 480 nm.

[f]Dominant component (associated to the monomer) of a bi-exponential decay; the additional decay time is of 0.81and 2.63 ns in acetonitrile and dichloromethane, respectively (see text for more details).

[g] $k_F = \phi_F / \tau_F$.

[h] $k_{NR} = (1 - \phi_F) / \tau_F$.

ND - not determined.

A more detailed observation shows, however, that the absorption spectrum of **L** is red-shifted and broader when compared with naphthalene itself [35].

The presence of a dimer becomes more evident in the fluorescence decay obtained with excitation at 281 nm and collected at 340 nm and 500 nm (*data not shown*). In this case the global (simultaneous) analysis of the decays at 340 and 500 nm leads bi-exponential decays with the same decay times at and different pre-exponential factors. It is worth reminding that the pre-exponential factors mirror the concentration at time zero of the associated species: the monomer and the dimer. Since the monomer emits preferentially at shorter wavelengths and the dimer at longer ones, the decay times should therefore be associated with a monomer species (shorter decay component) and dimeric (longer decay component). In addition, the absence of rising components (rise-time) suggests that the dimeric species is not formed in the excited state, but is already present in the ground state.

4
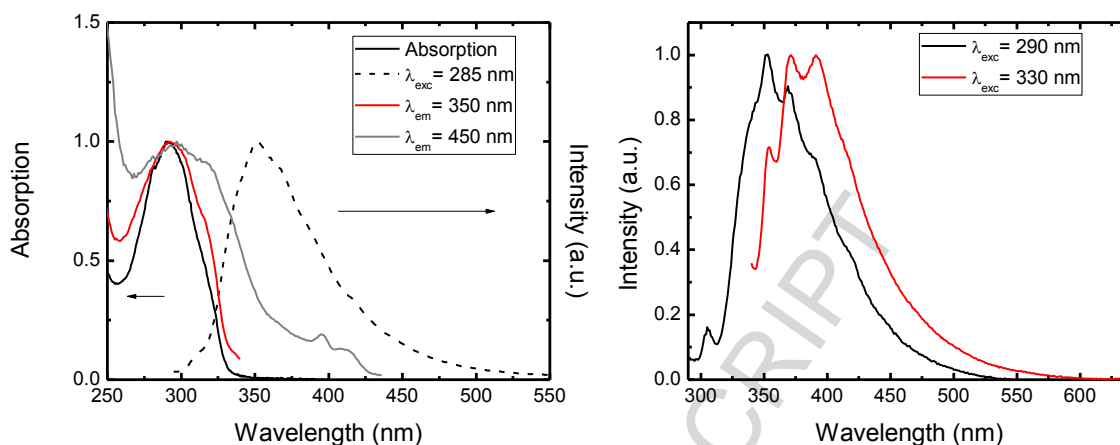
Figure 1. *From left to right.* Normalized absorption, emission (λ_{exc}= 285 nm) and excitation spectra (λ_{em}= 350 and 450 nm) and normalized emission (λ_{exc}= 290 and 330 nm) of **L** in acetonitrile.

Upon the addition of the metal ions Cu^{2+}, Zn^{2+}, Cd^{2+} and Hg^{2+} to an acetonitrile solution of **L** [36], the vibronic progression of the monomer band (Figure 2) changes, which is indicative of the formation of a complex involving the metal M and the ligand **L** (with its absorption beneath the emission spectra of the monomer).

Indeed, upon addition of different metal cations (M), a shift towards lower wavelengths in the absorption spectra likely due to a photoinduced charge transfer involving the metal and the ligand, MLCT [with sharp isosbestic points (Figure 2 right hand panels) at ~215, ~230, ~250 and ~325 nm and, more evident, at ~290 nm] together with a quenching of the vibronically resolved fluorescence band (maximum at ~352 nm) was observed (Figure 2). Indeed, when a fluorophore contains an electron-donating group (eg. an amino group) conjugated to an electron-withdrawing group, it undergoes intramolecular charge transfer from the donor to the acceptor upon excitation by light [37]. The amino group of **L** plays the role of electron donor (within the fluorophore) and interacts with the cation; the latter reduces the electron-donating ability of this group. This results in the stabilization of the HOMO and therefore a higher (HOMO-LUMO energy difference is obtained) leading to a blue shift of the absorption spectrum together with a decrease of the molar absorption coefficient (photoinduced charge transfer PCT) [38].

From Figure 2 it can also be seen that the change in intensity of the absorption (increase at 275 nm and decrease and 310 nm) and emission (decrease) spectra with the incremental addition of ligand is found non-linear. Again, this is likely a result from the presence of a dimer (resulting from the formation of a complex between the metal and the ligand **L**).

From Figure 2, it is also worth noting that the blue-shift in the absorption spectra upon addition of M seems to be independent on the nature of the metal. Moreover, with the addition of the metal M, the ratio of the vibronic bands is changed; this, however, does not show a linear dependence with the incremental addition of M and is likely indicative of the presence/increasing contribution of a dimer resulting from the formation of a complex between the ligand **L** and the metal M. Indeed, if the quenching effect were only due to an electron or energy transfer from **L** to M it would induce a decrease of the fluorescence band as a whole; in contrast, an equilibrium **L** $\leftrightarrow$ **ML** will

5

promote a gradual change in the absorption (perceptible in Figure 3
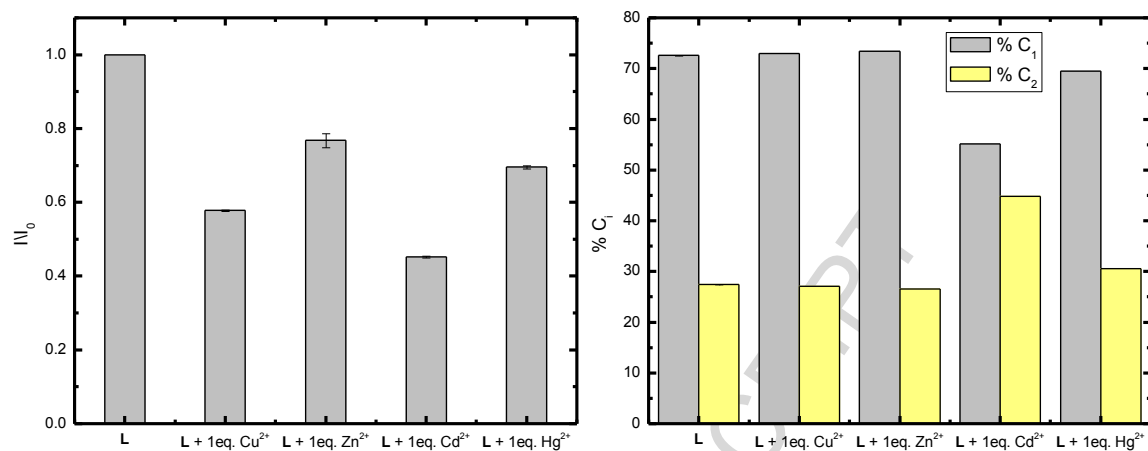
Figure 3) with a different contribution of **L** and M**L** at the excitation wavelength. This would produce a different ratio of the **L** and M**L** absorption and emission, which will induce a different vibronic progression of the (total) emission band.

Further and detailed knowledge can be obtained from time-resolved fluorescence experiments. As showed above the fluorescence decays were found to be bi-exponentials; see Table 1. The incremental addition of metal cation leads to non-significant changes on the decay time values. However, the same does not happen with the fractional fluorescence contribution of each species. The fractional contribution (C_i) of each species (when in presence of a bi- or higher order decays) is given by the following equation

$$C_i(\%) = \frac{a_i \tau_i}{\sum\limits_{i=1}^{n} a_i \tau_i} \times 100 \quad \textbf{Equation 1}$$

where n is the number of exponential terms, a_i represents the contribution of each exponential term at t= 0 and τ_i are the associated decay times.

6
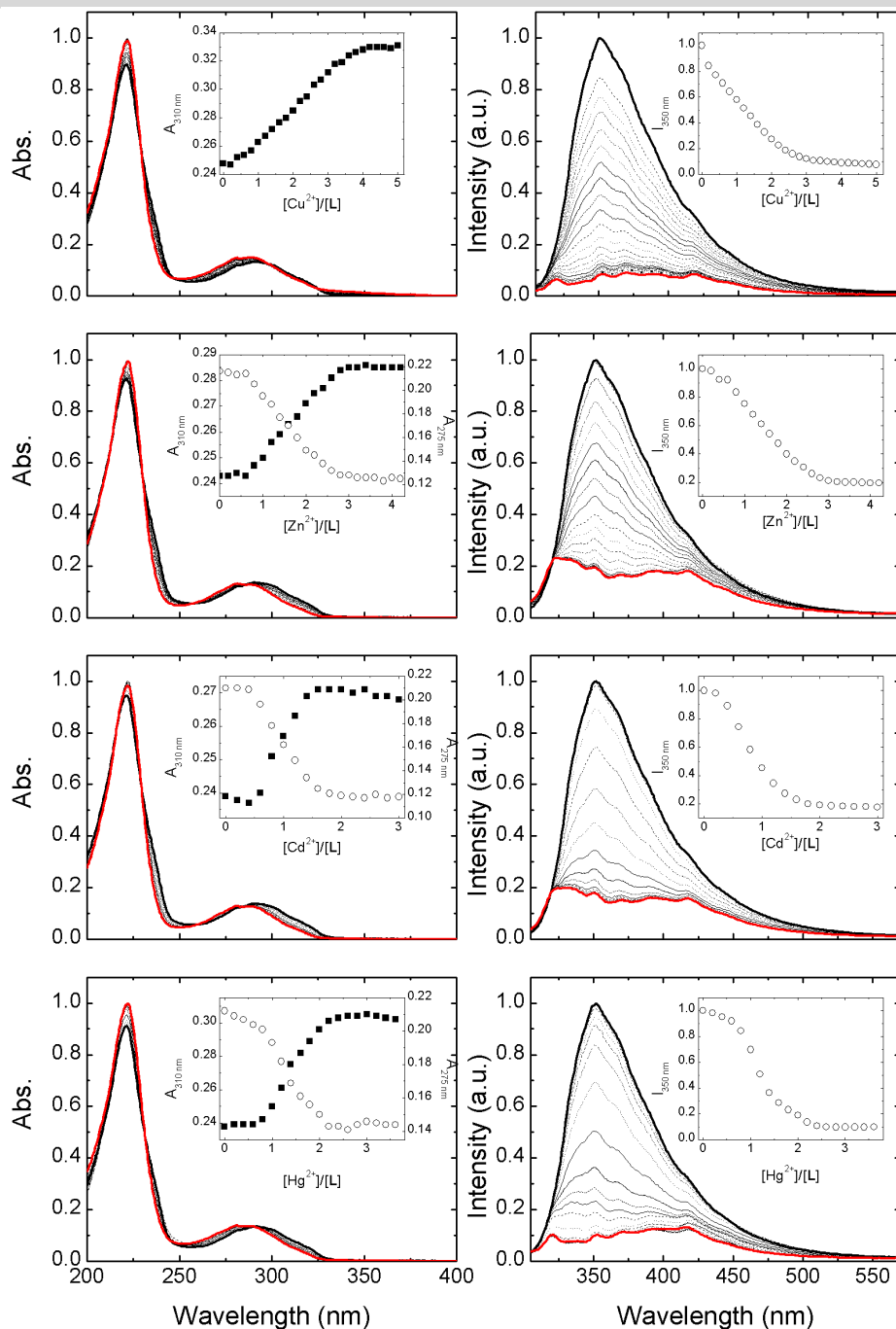
Figure 2. *From left to right*: Absorption and emission (λ_{exc}= 292 nm) spectra of **L** in acetonitrile with the addition of Cu^{2+}, Zn^{2+}, Cd^{2+} and Hg^{2+}. Inset from absorption: Representation of the absorption at 275 and 310 nm as a function of [M]/[**L**]. Inset from emission: Representation of the fluorescence intensity at 370 nm as a function of [M]/[**L**]. The bold black and red lines correspond, respectively to [M]/[**L**]= 0 and [M]/[**L**]= [M]/[**L**]$_{max}$. [M]/[**L**]$_{max}$= 3-5. [**L**]= 1×10^{-5} M.

From Figure 3 it can be seen that although the ratio I/I_0 is lower for the cadmium ion, the decrease is relatively small when compared to the other ions (from a I/I_0 ratio of 0.45 for Cd^{2+} to 0.77 for Zn^{2+}). However, in the case of the fractional contribution of the component 2 (associated to the longer decay time), there is a clear departure of the value of Cd^{2+} with the value of 45% relative to the general constancy

7

found for **L** alone, Cu^{2+} and Zn^{2+} and Hg^{2+} with a value of ~30%. Since the contributions of C_1 and C_2 mirror the ground state contributions of each species if the C_2 species decreases in contribution, the C_1 increases proportionally. Therefore for **L**:Cd^{2+} the value is now 55% vs. 70% for **L** alone and interacting with all the other metals.
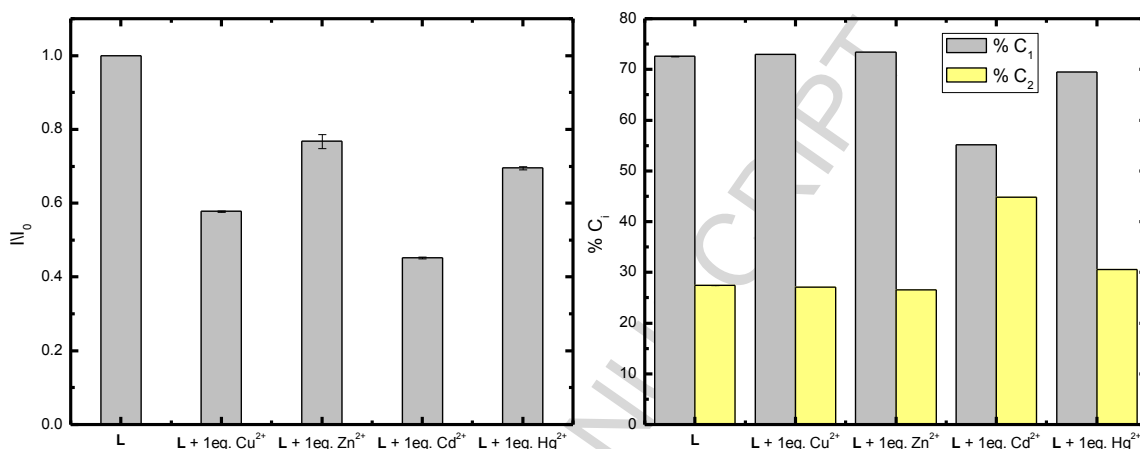
Figure 3. I/I_0 ratio (left hand panel) and $\%C_i$ (right hand panel) for free **L** in acetonitrile and in the presence of 1 equivalent of Cu^{2+}, Zn^{2+}, Cd^{2+} and Hg^{2+}.

The stability constants for the interaction of **L** with Cu^{2+}, Zn^{2+}, Cd^{2+} and Hg^{2+} were calculated using HypSpec software and are summarized in 2 [39]. Taking into account these values, the sequence of the strongest interaction expected for **L** decreases in the follow order: $Hg^{2+} > Cd^{2+} > Zn^{2+} > Cu^{2+}$.

Table 2. Stability constants for probe **L** in the presence of Cu^{2+}, Zn^{2+}, Cd^{2+} and Hg^{2+} in acetonitrile for an interaction 1:1 (Metal/Ligand).

Interaction (M:L)	Σ log β (Abs)	Σ log (Emission)
Cu^{2+} (1:1)	6.12 ± 0.01	6.34 ± 0.01
Zn^{2+} (1:1)	6.73 ± 0.01	6.84 ± 0.01
Cd^{2+} (1:1)	8.42 ± 0.01	8.38 ± 0.01
Hg^{2+} (1:1)	9.94 ± 0.01	9.97 ± 0.01

Conclusions

The spectral and photophysical characterization of a probe bearing two naphthalene units and its interaction with different metal ions (Zn^{2+}, Cu^{2+}, Cd^{2+} and Hg^{2+}) was undertaken in acetonitrile. In all cases a blue shift in the absorption spectra and a quenching fluorescence emission of the ligand was observed. From time-resolved it is shown that the ligand **L** show a higher affinity towards the metal ion cadmium in acetonitrile medium. Moreover, although probe **L** is apparently not selective for any of the metal ions studied, the different values of

8

I/I_0 and emission contributions (from time-resolved data) for each of the emissive species obtained allow differentiating between Zn^{2+}, Cu^{2+}, Cd^{2+} and Hg^{2+}.

Abbreviations

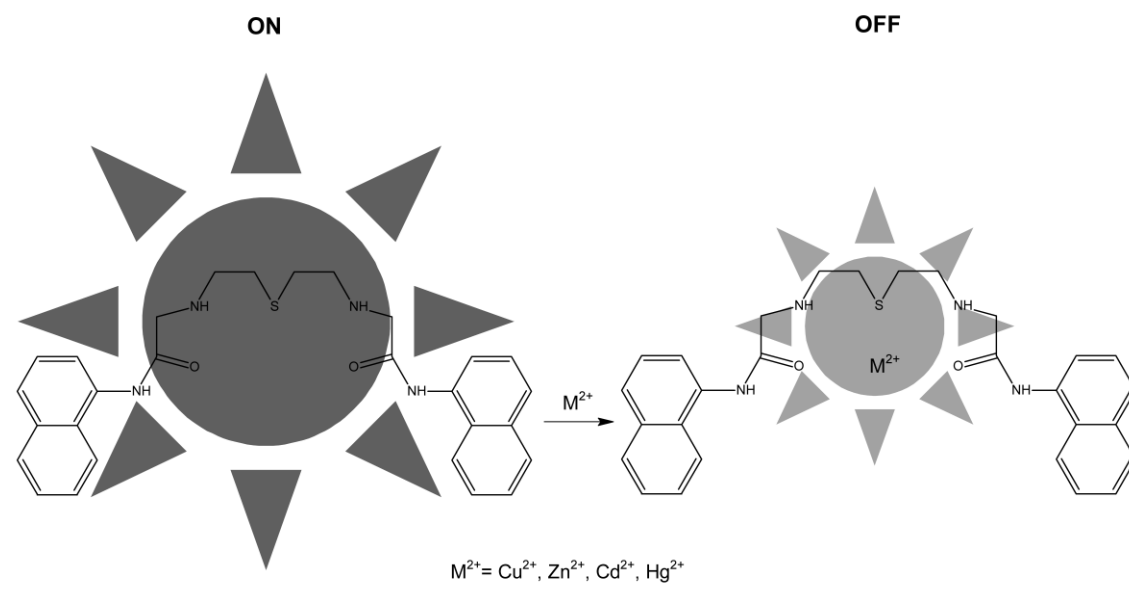A. C., autocorrelation, **L**, ligand; M, metal; ps, picosecond, TCSPC, time-correlated single photon counting.

References

Graphical Abstract

ON **OFF**

M²⁺= Cu²⁺, Zn²⁺, Cd²⁺, Hg²⁺

Synopsis

Synthesis of Cu^{2+}, Zn^{2+}, Cd^{2+} and Hg^{2+} solid metal complexes derivatives from **L**. Photophysical properties of **L** and study of the M:**L** complex in acetonitrile solution.

Bi-exponential fluorescence decay of **L** in dichloromethane: monomeric and dimeric species.

Highlights

Synthesis of Cu^{2+}, Zn^{2+}, Cd^{2+} and Hg^{2+} solid metal complexes derivatives from **L**. Photophysical properties of **L** and study of the metal complexation properties in acetonitrile solution.

Bi-exponential fluorescence decay of **L** in dichloromethane: monomeric and dimeric species.

[1] J.Y. Choi, D. Kim, J. Yoon, Dyes and Pigments 96 (2013) 176-179.

[2] R. Martínez, A. Espinosa, A. Tárraga, P. Molina, Tetrahedron 66 (2010) 3662-3667.

[3] C.D. Geddes, J.R. Lakowicz, Advanced Concepts in Fluorescence Sensing, 2005.

[4] L. Basabe-Desmonts, D.N. Reinhoudt, M. Crego-Calama, Chem. Soc. Rev. 36 (2007) 993-1017.

[5] B. Hu, P. Lu, Y. Wang, New J. Chem. 37 (2013) 1645-1653.

[6] F. Pina, J.C. Lima, C. Lodeiro, J.S. Seixas de Melo, P. Diaz, M.T. Albelda, E. García-España, J. Phys. Chem. A 106 (2002) 8207-8212.

[7] B. Valeur, Molecular Fluorescence - Principles and Applications, WILEY-VCH, 2002.

[8] J.S. Seixas de Melo, T. Costa, C.S. de Castro, A.L. Maçanita, "Photophysics of fluorescently labeled oligomers and polymers" in Specialist Periodic Reports in Photochemistry, Ed. Angelo Albini and Elisa Fasani, 2013, 41, 59-126.

[9] J. Fernández-Lodeiro, C. Nuñez, C.S. de Castro, E. Bértolo, J.S. Seixas de Melo, J.L. Capelo, C. Lodeiro, Inorg. Chem. 52 (2013) 121-129.

[10] J. B. Birks, Photophysics of Aromatic Molecules, Wiley Intersience, 1970.

[11] J.R. Lackowicz, Principles of Fluorescence Spectroscopy, 3rd Edition, Springer, 2006.

[12] J. Pina, J.S. Seixas de Melo, D. Breusov, U. Scherf , Phys. Chem. Chem. Phys. 15 (2013) 15204 -15213.

[13] S. Goswami, A.K. Das, S. Maity, Dalton Trans. 42 (2013) 16259-16263.

[14] J.S. Seixas de Melo, R. Rondão, H.D. Burrows, M.J. Melo, S. Navaratnam, R. Edge, G. Voss, Chem. Phys. Chem. 7 (2006) 2303-.

[15] J.S. Seixas de Melo, J. Pina, F.B. Dias, A.L. Maçanita, Experimental Techniques for Excited State Characterisation, Chapter 15, pages 533-585, in Applied Photochemistry, R. C. Evans, P. Douglas, H. D. Burrows (Eds.), Springer, 2013.

[16] J.S. Seixas de Melo, J. Pina, F.B. Dias, A.L. Maçanita, Applied Photochemistry (2013) 533-585.

[17] P. Jiang, L. Chen, J. Lin, Q. Liu, J. Ding, X. Gao, Z. Guo, Chem. Commun., (2002) 1424-1425.

[18] F.-G. Bănică, Chemical Sensors and Biosensors, John Wiley & Sons, Ltd, 2012, pp. 1-20.

[19] D.B.G. Williams, M. Lawton, J. Org. Chem., 75 (2010) 8351-8354.

[20] C. Lodeiro, J.C. Capelo, J.C. Mejuto, E. Oliveira, H.M. Santos, B. Pedras, C. Núñez, Chem. Soc. Rev. 39 (2010) 2948-2976.

[21] I.B. Berlman, Handbook of Fluorescence Spectra of Aromatic Molecules, in, Academic Press, N.Y., 1971.

[22] A.M.G. Silva, Carla Queirós, F. Monteiro-Silva, Naphthalene-Based Fluorophores: Structure, Properties and Applications, in, pp. 153-180.

[23] L. Fernandes, M. Boucher, J. Fernández-Lodeiro, E. Oliveira, C. Núñez, H.M. Santos, J.L. Capelo, O.N. Faza, E. Bértolo, C. Lodeiro, Inorg. Chem. Commun. 12 (2009) 905-912.

[24] C. Lodeiro, F. Pina, Coord. Chem. Rev. 253 (2009) 1353-1383.

[25] E. Oliveira, C. Núñez, B. Rodríguez-González, J.L. Capelo, C. Lodeiro, Inorg. Chem. 50 (2011) 8797-8807.

[26] J. Fernández-Lodeiro, C. Núñez, R. Carreira, H.M. Santos, C. Silva López, J.C. Mejuto, J.L. Capelo, C. Lodeiro, Tetrahedron 67 (2011) 326-333.

[27] L. Fernandes, M. Boucher, J. Fernández-Lodeiro, E. Oliveira, C. Nuñez, H.M. Santos, J.L. Capelo, O.N. Faza, E. Bértolo, C. Lodeiro, Inorg. Chem. Commun. 12 (2009) 905-912.

[28] C. Núñez, M. Mato-Iglesias, R. Bastida, A. Macías, P. Pérez-Lourido, C. Platas-Iglesias, L. Valencia, Eur. J. Inorg. Chem. (2009) 1086-1095.

[29] C. Núñez, R. Bastida, A. Macias, C. Lodeiro, L. Valencia, Inorg. Chim. Acta 362 (2009) 3454-3460.

[30] C. Núñez, R. Bastida, A. Macías, L. Valencia, N.I. Neuman, A.C. Rizzi, C.D. Brondino, P.J. González, J.L. Capelo, C. Lodeiro, Dalton Trans. 39 (2010) 11654-11663.

[31] A. Fernández-Lodeiro, J. Fernández-Lodeiro, C. Núñez, Rufina Bastida, J.L. Capelo, C. Lodeiro, Chemistry Open 2 (2013) 200-207.

[32] **Synthesis of the Metal Complexes of L.** *General Procedure.* A solution of the appropriate metal salt (0.021 mmol) in absolute ethanol (5 mL) was added dropwise to a stirred solution of ligand **L** (0.010 g, 0.021 mmol) in the same solvent (20 mL). The solution was stirred for 4h at 150ºC, and the solvent was partially removed to *ca.* 5 mL. In all cases, the formation of an initial precipitate was observed from the treatment of the remaining solutions with diethyl ether. The solid metal complexes were isolated from the evaporation of the leftover solutions. Cu^{2+} *complex*: formula **[CuL(CF$_3$O$_3$S)$_2$].4H$_2$O** Anal. Calcd for CuC$_{30}$H$_{38}$F$_6$N$_4$O$_{12}$S$_3$ (MW: 919.08): C, 39.2; H, 4.2; N, 6.0; S, 10.4. Found: C, 39.8; H, 4.5; N, 6.1; S, 10.8. Yield: 55%. IR (cm^{-1}): ν= 1426 (C=C)ar, 1660 (C=O), 2982 (N-H). MALDI-MS (*m/z*): 549.27 [CuL]$^+$. Zn^{2+} *complex*: formula **[ZnL(CF$_3$O$_3$S)$_2$].6H$_2$O**. Anal. Calcd for ZnC$_{30}$H$_{42}$F$_6$N$_4$O$_{14}$S$_3$ (MW: 956.11): C, 37.6; H, 4.4; N, 5.8; S, 10.0. Found: C, 37.7; H, 4.5; N, 5.4; S, 9.6. Yield: 47%. IR (cm^{-1}): ν= 1428 (C=C)ar, 1664 (C=O), 2976 (N-H). MALDI-MS (*m/z*): 551.28 [ZnL]$^+$. Cd^{2+} *complex*: formula **[CdL(CF$_3$O$_3$S)$_2$].6H$_2$O**. Anal. Calcd for CdC$_{30}$H$_{42}$F$_6$N$_4$O$_{14}$S$_3$ (MW: 1006.08): C, 35.8; H, 4.2; N, 5.5; S, 9.5. Found: C, 35.9; H, 3.9; N, 5.2; S, 9.8. Yield: 31 %. IR (cm^{-1}): ν= 1428 (C=C)ar, 1660 (C=O), 2978 (N-H). MALDI-MS (*m/z*): 599.01 [CdL]$^+$. Hg^{2+} *complex*: formula **[HgL(CF$_3$O$_3$S)$_2$].4H$_2$O**. Anal. Calcd for HgC$_{30}$H$_{38}$F$_6$N$_4$O$_{12}$S$_3$ (MW: 1058.13): C, 34.1; H, 3.6; N, 5.3; S, 9.1. Found: C, 34.4; H, 3.5; N, 5.0; S, 8.8. Yield: 33 %. IR (cm^{-1}): ν= 1430 (C=C)ar, 1666 (C=O), 2980 (N-H). MALDI-MS (*m/z*): 688.53 [HgL]$^+$, 734.59 [HgL(C$_2$H$_6$O)]$^+$.

[33] Elemental analyses were carried out at the REQUIMTE DQ Service (Universidade Nova de Lisboa), on a Thermo Finnigan-CE Flash-EA 1112-CHNS instrument. Infra-red spectra were recorded on a Perkin Elmer FT-IR spectrometer. Matrix-assisted laser desorption ionization time-of-flight mass spectrometry (MALDI-TOF-MS) analysis was performed in a MALDITOF-MS model Bruker Ultraflex II workstation equipped with a nitrogen laser radiating at 337 nm from Bruker (Germany). The spectra represent accumulations of 5×100 laser shots. The reflectron mode was used. The ion source and flight tube pressures were less than $1.80×10^{-7}$ and $5.60×10^{-7}$ Torr, respectively. The MALDI-MS spectra of the metal complexes (1 or 2 mg/mL) were recorded using the conventional sample preparation method for MALDI-MS.

[34] **Spectrophotometric and spectrofluorimetric measurements:** The UV-Vis absorption spectra were obtained using a Shimadzu 2450 UV-Vis spectrophotometer; fluorescence spectra were recorded on Horiba Jobin-Yvon SPEX Fluorolog 3-22 or Fluoromax 4 spectrometers. All the fluorescence spectra were corrected for the wavelength response of the system. The fluorescence decays of the compounds were obtained with picosecond resolution (ps-TCSPC) with the equipment described elsewhere [J. Pina, J. Seixas de Melo, H.D. Burrows, A.L. Maçanita, F. Galbrecht, T. Bünnagel, U. Scherf, Macromolecules, 42 (2009) 1710-1719] and were analyzed using the method of modulating functions implemented by Striker et al. [G. Striker, V. Subramaniam, C.A.M. Seidel, A. Volkmer, J. Phys. Chem. B, 103 (1999) 8612-8617]. The experimental excitation pulse [full width at half maximum (fwhm)= 21 ps] was measured using a LUDOX scattering solution in water. After deconvolution of the experimental signal, the time resolution of the apparatus was ca. 2 ps. The fluorescence quantum yield for **L** in dichloromethane was determined using a solution of α_3 in ethanol as a reference (ϕ_F= 0.054).

[35] M. Montalti, A. Credi, L. Prodi, M.T. Gandolfi, Handbook of Photochemistry, Taylor and Francis, 2006.

[36] All spectroscopic titrations were performed (at 293 K) as follows: (i) a solution of the ligand was prepared by dissolving an appropriate amount of the ligand in acetonitrile and diluted to the desired concentration ([**L**]= 1×10^{-5} M); (ii) titrations were carried out by the addition of microliter amounts of standard solutions of the ions dissolved in acetonitrile ([M]= 10^{-4}-10^{-3} M); (iii) 3 ml of the solution was placed to a 1 cm quartz cuvette. To acquire the fluorescence spectra relatively fast (yet with sufficient resolution), an integration time of 0.1 s was used and in order to homogenize the solution manual agitation was performed after each addition of metal and before running the absorption or emission spectrum.

[37] F. Pina, J.C. Lima, C. Lodeiro, J. Seixas de Melo, P. Díaz, M.T. Albelda, E. García-España, J. Phys. Chem. A 106 (2002) 8207-8212.

[38] B. Valeur, J.-C. Brochon, New Trends in Fluorescence Spectroscopy: Applications to Chemical and Life Sciences, Springer, 2001.

[39] P. Gans, A. Sabatini, A. Vacca, Talanta 43 (1996) 1739-1753.